

See discussions, stats, and author profiles for this publication at: <https://www.researchgate.net/publication/224002160>

# Stringing up the Pearls: Self-Assembly, Optical and Electronic Properties of CdSe- and Au-LiMo<sub>3</sub>Se<sub>3</sub> Nanoparticle-Nanowire Composites

## ARTICLE

---

CITATIONS

21

---

READS

19

## 4 AUTHORS, INCLUDING:



Frank Osterloh

University of California, Davis

114 PUBLICATIONS 3,954 CITATIONS

SEE PROFILE

# Stringing up the Pearls: Self-Assembly, Optical and Electronic Properties of CdSe– and Au–LiMo<sub>3</sub>Se<sub>3</sub> Nanoparticle–Nanowire Composites

Frank E. Osterloh,\* Jason S. Martino, Hiroki Hiramatsu, and Daniel P. Hewitt

*Department of Chemistry, University of California, One Shields Avenue, Davis, California 95616*

*Received August 7, 2002; Revised Manuscript Received November 18, 2002*

## ABSTRACT

Chevrel-type LiMo<sub>3</sub>Se<sub>3</sub> nanowires dissolved in dimethyl sulfoxide were decorated with 13 nm citrate ligated Au particles (water) and 6 nm trioctylphosphineoxide ligated CdSe particles (tetrahydrofuran) by combining the respective solutions at room temperature, followed by mild acidification with hydrochloric acid in the case of Au. The morphology of the formed nanostructured Au–LiMo<sub>3</sub>Se<sub>3</sub> and CdSe–LiMo<sub>3</sub>Se<sub>3</sub> aggregates depends on stoichiometry and reaction conditions. While the UV/vis spectra of the aggregates are largely the sum of the subspectra of the building blocks, the emission spectra of the CdSe–LiMo<sub>3</sub>Se<sub>3</sub> material reveal quenching of CdSe based photoluminescence. The electrical conductance of 5 nm thick films obtained by drying solutions of the composites decreases with increasing temperature, which shows that the nanowires remain metallic after binding of the nanoparticles.

Electrically conducting organic or inorganic nanowires are generally regarded as crucial building blocks of future microelectronics.<sup>1</sup> Of the many known varieties, LiMo<sub>3</sub>Se<sub>3</sub> nanowires<sup>2</sup> obtained after cation exchange and exfoliation of the Chevrel compound InMo<sub>3</sub>Se<sub>3</sub><sup>3</sup> are remarkable in several respects: As condensation polymers of triangular Mo<sub>3</sub>Se<sub>3</sub> units, these molecular wires have a diameter of only 0.85 nm (from crystal data),<sup>4</sup> which makes them smaller than single (1–2 nm) and multiwalled (2–25 nm) carbon nanotubes.<sup>5</sup> Bundles of LiMo<sub>3</sub>Se<sub>3</sub> wires possess metallic conductivity<sup>6,7</sup> and are soluble in polar organic solvents, which enables a solution manipulation of the wires using soft chemistry methods. The successful incorporation of LiMo<sub>3</sub>Se<sub>3</sub> nanowires into an organic polymer was reported in 1995 by DiSalvo's group.<sup>8</sup> Later, Yang and co-workers encapsulated LiMo<sub>3</sub>Se<sub>3</sub> wires with organic surfactants to yield organic–inorganic hybrid materials,<sup>9</sup> and very recently the same group also employed the wires as sacrificial templates for the synthesis of gold nanowires.<sup>10</sup> Here, we report a solution phase method for using LiMo<sub>3</sub>Se<sub>3</sub> nanowires to “wire up” metallic Au and semiconducting CdSe nanoparticles. The resultant nanostructured composites are soluble in organic solvents and form electrically conducting films when deposited from solution. The integration of nanoparticles into conducting networks is of great technological interest; potential applications for these and related inorganic composites exist in areas ranging from photochemical cells<sup>11,12</sup> and batteries to nanowire based chemical sensors<sup>13–15</sup> and electrochemical catalysts.

Syntheses were carried out at room temperature in a nitrogen glovebox in degassed and/or dried solvents. Aqueous solutions of citrate ligated gold particles were prepared as previously described,<sup>16</sup> diluted with ultrapure water ( $R > 18 \text{ M}\Omega$ ) to a gold content of  $0.50 \times 10^{-3} \text{ mol/L}$ , and purged with nitrogen before use. Trioctylphosphineoxide (TOPO) ligated CdSe particles (6 nm) were synthesized according to Peng's method.<sup>17</sup> InMo<sub>3</sub>Se<sub>3</sub> was prepared and cation-exchanged with LiI according to DiSalvo.<sup>4</sup> A  $1.73 \times 10^{-3} \text{ M}$  stock solution of LiMo<sub>3</sub>Se<sub>3</sub> was prepared by dissolving 23 mg of LiMo<sub>3</sub>Se<sub>3</sub> in 25 mL of dimethyl sulfoxide (DMSO) with sonication. Optical measurements were performed in sealed quartz ampules, using Hewlett-Packard 8450A UV/vis and Perkin-Elmer LS50B luminescence spectrometers. Samples for electron microscopy (SEM, FEI XL30-SFEG; TEM, Hitachi H-600) were prepared using silicon wafers or holey carbon coated TEM grids as supports.

## Experimental Section

**Synthesis of CdSe·TOPO/LiMo<sub>3</sub>Se<sub>3</sub>.** (a) A stock solution of trioctylphosphineoxide (TOPO) ligated CdSe particles (6 nm) was prepared by dissolving 75 mg of solid CdSe·TOPO in 20 mL of THF. A 0.4 mL volume of this solution was added with stirring to 0.75 mL of the  $1.73 \times 10^{-3} \text{ M}$  LiMo<sub>3</sub>Se<sub>3</sub> stock solution in dimethyl sulfoxide (DMSO). The clear brown-red solution was sonicated for 30 s, and the product precipitated by adding 3 mL of ether. The brown precipitate was centrifuged off, washed with tetrahydrofuran (THF), and then dispersed in 2 mL of THF with sonication. (b) For the

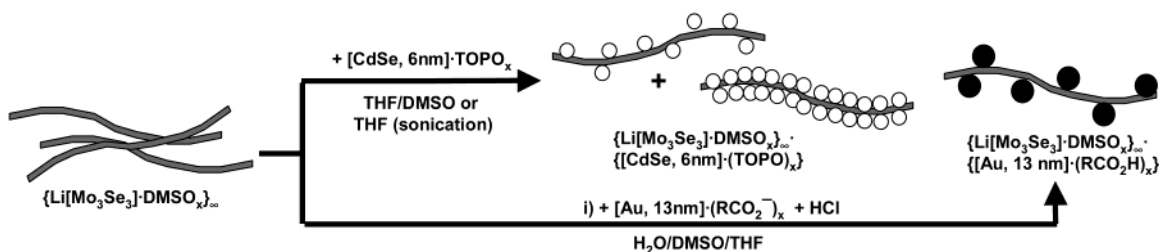


**Figure 1.** Synthesis of the composites.

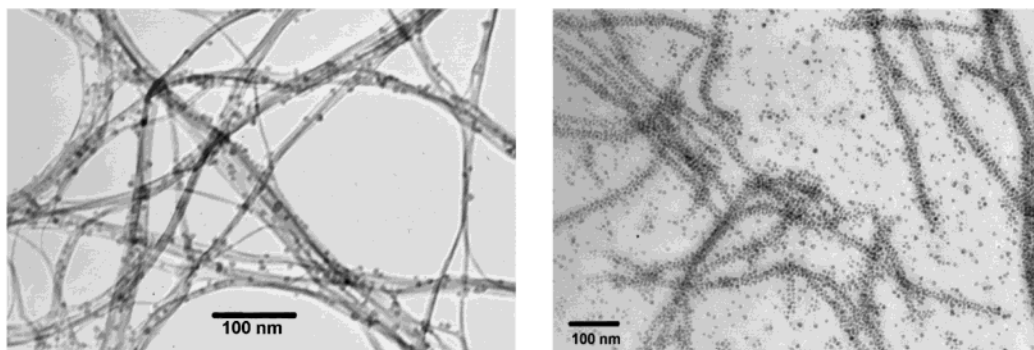


**Figure 2.** Transmission electron micrographs of two samples of CdSe·LiMo<sub>3</sub>Se<sub>3</sub> synthesized according to methods (a) and (b) (Experimental Section).

photoluminescence measurements, a DMSO-free batch of CdSe·TOPO/LiMo<sub>3</sub>Se<sub>3</sub> was prepared in THF, because the PL of CdSe·TOPO particles is partially quenched in the presence of high concentrations of DMSO. LiMo<sub>3</sub>Se<sub>3</sub> nanowires were first precipitated by combining 0.5 mL of the stock solution with 4 mL of THF, and washed three times with 4 mL of THF to remove any unbound DMSO. The wires were suspended in 4.0 mL of THF and 1.0 mL of the CdSe·TOPO stock solution in THF was added. The suspension was sonicated (5 min) until a homogeneous mixture was formed. The solid was isolated by centrifugation, washed two times with THF, and dispersed in THF (for PL spectrum) or MeOH (to make a film).

**Synthesis of Au·cit/LiMo<sub>3</sub>Se<sub>3</sub>.** To 0.2 mL of the LiMo<sub>3</sub>Se<sub>3</sub> nanowire stock solution in DMSO was added 3 mL of an aqueous solution of 13 nm gold colloid ( $0.50 \times 10^{-3}$  mol Au/L) with stirring to yield a clear red solution. The mixture was sonicated for 30 s, and 0.1 mL (150 equiv of HCl per mole of LiMo<sub>3</sub>Se<sub>3</sub>) of a 0.6 M HCl solution in THF was then slowly added with stirring. The red precipitate was centrifuged off, and the colorless supernatant was discarded. The product was dispersed in 2 mL of MeOH with sonication to yield an optically clear red solution that was stable for several minutes, depending on concentration of the composite. Stable solutions of the composite form in DMSO or water.

## Results and Discussion

CdSe·TOPO–LiMo<sub>3</sub>Se<sub>3</sub> composites of varying compositions were synthesized (Figure 1) by combining solutions of trioctylphosphine (TOPO) ligated cadmium selenide particles (6 nm in THF)<sup>17</sup> with a solution of exfoliated LiMo<sub>3</sub>Se<sub>3</sub> nanowires in DMSO, or by sonicating a mixture of CdSe·TOPO in THF with LiMo<sub>3</sub>Se<sub>3</sub> freshly precipitated from

DMSO by addition of THF. These reactions afford CdSe–LiMo<sub>3</sub>Se<sub>3</sub> composites as brown-red solids that can easily be dissolved in methanol or THF to give optically clear solutions.

Gold–LiMo<sub>3</sub>Se<sub>3</sub> nanowire composites were similarly synthesized by mixing citrate ligated gold particles (13 nm in water)<sup>16</sup> and LiMo<sub>3</sub>Se<sub>3</sub> in DMSO and after adding 60  $\mu$ mol of hydrochloric acid (150 mole equiv based on LiMo<sub>3</sub>Se<sub>3</sub>), dissolved in THF. The role of the acid is to reduce the negative charges on both wires and gold particles via protonation, to eliminate repulsive Coulomb forces which do inhibit the formation of a composite. The gold–LiMo<sub>3</sub>Se<sub>3</sub> composite forms stable red solutions in polar solvents such as DMSO or water.

The morphology of the CdSe–wire composites depends on the method of synthesis and on their composition. Transmission electron micrographs of samples synthesized in homogeneous and in heterogeneous reactions are shown in Figure 2. When the CdSe content is low, the network formed by bundles of the LiMo<sub>3</sub>Se<sub>3</sub> polymer remains mostly intact. Most of the wire bundles in the network are 3–4 nm thick (measured by AFM, see Supporting Information) and contain 7–13 LiMo<sub>3</sub>Se<sub>3</sub> strands (assuming hdp of LiMo<sub>3</sub>Se<sub>3</sub> molecular chains). The CdSe particles are randomly scattered over this wire network, mostly as individual particles but occasionally in the form of clusters. The CdSe–LiMo<sub>3</sub>Se<sub>3</sub> composite synthesized in the heterogeneous reaction with an excess of CdSe nanoparticles contains LiMo<sub>3</sub>Se<sub>3</sub> wires that are entirely and uniformly covered with CdSe particles (Figure 2b). Here the nanowires can be viewed as structural templates for the anisotropic aggregation of the CdSe particles.

The morphology of the gold–wire composite (Figure 3), resembles the low-coverage CdSe–LiMo<sub>3</sub>Se<sub>3</sub> composite.

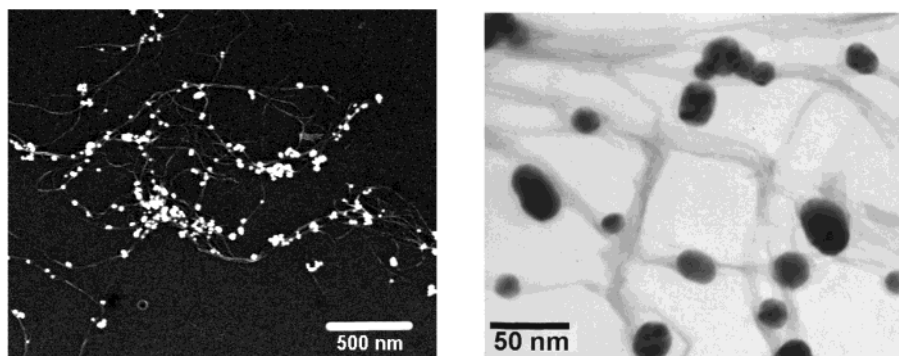


**Figure 3.** Scanning electron (a) and transmission electron micrographs (b) of Au-LiMo<sub>3</sub>Se<sub>3</sub> composite.

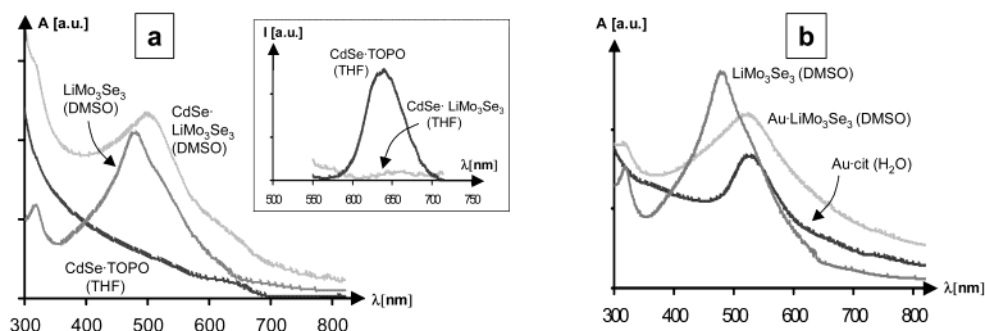


**Figure 4.** Electronic spectra and PL spectra (insert) of (a) CdSe-LiMo<sub>3</sub>Se<sub>3</sub> and (b) Au-LiMo<sub>3</sub>Se<sub>3</sub> composites in the indicated solvents.

However, the LiMo<sub>3</sub>Se<sub>3</sub> network is less regular, probably because of the larger structure directing influence of the 13 nm Au particles, whose surface area is about five times that of the 6 nm CdSe particles. As a result of the stronger wire-particle bonding, gold particles are partially incorporated into bundles (Figure 3b), causing the observed morphology changes of the wire network.

Repeated washings of the composites with THF (CdSe-LiMo<sub>3</sub>Se<sub>3</sub>) and methanol or water (Au-LiMo<sub>3</sub>Se<sub>3</sub>) have no effect on the composition of the materials. The notions that CdSe-TOPO and LiMo<sub>3</sub>Se<sub>3</sub> lack bridging ligands, and further, that Lewis-hard Fe(II,III) ions of bare Fe<sub>3</sub>O<sub>4</sub> nanoparticles do not bind to the wires (unpublished results), are in support of a covalent bonding model. Strong covalent bonds can be formed by the Lewis-Soft couples cadmium(II)/selenide and Au(I) ions/selenide. The LiMo<sub>3</sub>Se<sub>3</sub> strands in the bundles, on the other hand, are held together electrostatically as in crystalline LiMo<sub>3</sub>Se<sub>3</sub>.

UV/vis spectra of the composites and their pure components are shown in Figure 4. The electronic spectra of both composites are mainly a superposition of the spectra of the separate building blocks. This suggests that LiMo<sub>3</sub>Se<sub>3</sub> nanowires and CdSe and Au particles remain intact after formation of the composite. The red color of the CdSe-LiMo<sub>3</sub>Se<sub>3</sub> and Au-LiMo<sub>3</sub>Se<sub>3</sub> composites originates from intense bands at 498 and 522 nm, respectively. For the pure wires, this weakly solvent-dependent band appears at 480 nm in DMSO, at 470 nm in H<sub>2</sub>O, and at 486 nm in propylenecarbonate. The shoulder at 640 nm in the CdSe-LiMo<sub>3</sub>Se<sub>3</sub> composite corresponds to the band gap excitation of CdSe nanoparticles (1.93 eV); its width reflects the size distribution of the 6 nm CdSe nanoparticles. In the UV/vis spectrum of the Au-LiMo<sub>3</sub>Se<sub>3</sub> composite, this feature is

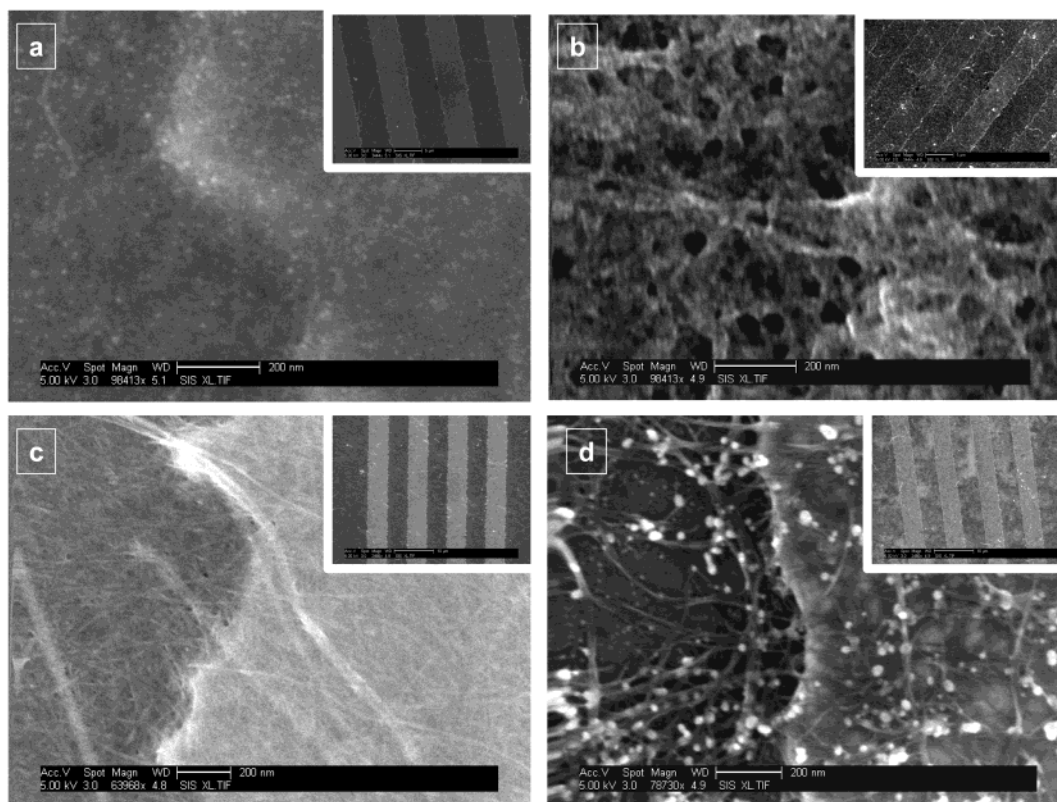
replaced with the surface plasmon band of the gold particles, which occurs at 526 nm for the pure gold colloid in water.

Photoluminescence spectra of CdSe-TOPO particles and of the CdSe-LiMo<sub>3</sub>Se<sub>3</sub> composite, prepared in THF, are shown in the inset of Figure 4a. When excited at 380 nm, solutions of TOPO-ligated CdSe particles in THF emit at 640 nm. Upon binding to the wires, this photoluminescence is quenched completely. Quenching can result from either TOPO removal (which allows surface redox processes to occur),<sup>18</sup> from injection of the photoexcited electrons into the LiMo<sub>3</sub>Se<sub>3</sub> polymer, or from dipolar coupling between nanoparticles and wires (Förster transfer).<sup>19</sup> Based on IR-spectroscopy, the first possibility can be ruled out. IR spectra of the composite (Supporting Information) clearly contain bands (2921 [CH<sub>2</sub>], 2854 [CH<sub>3</sub>] cm<sup>-1</sup>) characteristic of the TOPO ligands, the majority of which remain coordinated to the CdSe particles upon formation of the composite. Further measurements are required in order to determine the exact nature of the quenching in these systems.

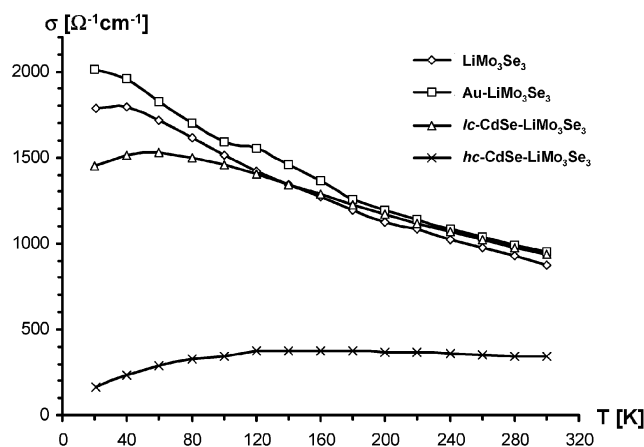
To determine the temperature-dependent electrical conductivity, films of the nanocomposites and of the pure nanowires were made by drop-coating 0.1–0.16 mL of the respective sample solutions (from methanol) onto a four-probe gold microelectrode array on borosilicate glass (gold leads: 5 μm (w) × 3 mm (l) × 110 nm (d); gaps: 5 μm), followed by evaporation of the solvent. This yielded films of 5 nm thickness, based on SEM (Figure 5) and AFM (Supporting Information) measurements.

Figure 6 shows plots of the electrical conductivities of the films versus temperature. Apart from the material with the highest CdSe content, all nanocomposites exhibit room-temperature conductivities on the order of 10<sup>3</sup> Ω<sup>-1</sup> cm<sup>-1</sup>, which agrees with theoretical calculations for exfoliated





**Figure 5.** Scanning electron micrographs of composite films on the gold microelectrode array (low magnification images are shown as insets; scale bars are 5–10  $\mu\text{m}$ ). The gold microelectrodes (on right side in each micrograph) are elevated by 110 nm over the borosilicate glass substrate. (a) CdSe–LiMo<sub>3</sub>Se<sub>3</sub> composites with low and (b) with high CdSe content, (c) pure LiMo<sub>3</sub>Se<sub>3</sub> nanowires, and (d) Au–LiMo<sub>3</sub>Se<sub>3</sub> composite (all from methanol).



**Figure 6.** Plots of the film conductance vs temperature. The specific conductivities were calculated based on a lead separation of 5  $\mu\text{m}$ , film length of 1 mm, and film thickness of 5 nm. For the Au–LiMo<sub>3</sub>Se<sub>3</sub> a film thickness of 3.5 nm was used in order to correct for the lower density of the film (see Figure 5d). The current was 1 mA. The abbreviations *lc* and *hc* refer to low and high CdSe content. Ohmic behavior was confirmed at all temperatures.

LiMo<sub>3</sub>Se<sub>3</sub> wires (100–1000  $\Omega^{-1} \text{cm}^{-1}$ ).<sup>8</sup> The electrical conductivity of the composite with high CdSe content is much lower because LiMo<sub>3</sub>Se<sub>3</sub> nanowires are entirely coated with a nearly insulating layer of CdSe (0.5  $\Omega^{-1} \text{cm}^{-1}$  for single crystals).<sup>20</sup> This layer increases the contact resistance between individual wire fragments in the film (see below).

The temperature behaviors observed for the films fall into two groups. Films of LiMo<sub>3</sub>Se<sub>3</sub> and of the Au–LiMo<sub>3</sub>Se<sub>3</sub>

material are metallic conductors over the entire temperature interval, a behavior that has been previously observed for individual wire bundles.<sup>7</sup> Films of the CdSe–LiMo<sub>3</sub>Se<sub>3</sub> composites, on the other hand, display metallic character only at high temperature, whereas below 60 K (low CdSe content) and 120 K (high CdSe content) the films become semiconducting. The semiconducting behavior indicates that charge transport across the film is limited by thermally activated hopping of electrons between nanoscale components.<sup>21</sup> This conduction mechanism has been previously observed by Murray et al. in gold nanoparticle films,<sup>22</sup> by Heath et al. for films of Ag nanocrystals,<sup>23</sup> and by DiSalvo in LiMo<sub>3</sub>Se<sub>3</sub> films, under conditions where the separation of the electrodes was much larger than the mean nanowire length.<sup>24,25</sup> Thermally activated conduction is most prominent for the CdSe containing films, because the introduction of this bad electrical conductor increases the electron tunneling barriers between separate nanowire bundles. The fact that at  $T > 120 \text{ K}$  even the CdSe–LiMo<sub>3</sub>Se<sub>3</sub> nanocomposite with the highest CdSe content behaves as a metallic conductor implies that conduction predominantly occurs through LiMo<sub>3</sub>Se<sub>3</sub> wire bundles, and not through CdSe nanoparticles.

In conclusion, we have shown that well-defined nanoparticle–nanowire composites can be synthesized in high yield by combining solutions of exfoliated LiMo<sub>3</sub>Se<sub>3</sub> nanowires with CdSe and Au colloids. Binding of the nanoparticles does not change the metallic properties of the nanowires, whose specific conductance stays close to the value for the pure

wires. Thus, nanowires of  $\text{LiMo}_3\text{Se}_3$  are well suited as electrical connects in nanostructured films. Because of its simplicity, the described wiring-up procedure may be of interest for the development of systems in which efficient charge transport to and from nanoparticles is a requirement, e.g., in batteries, solar cells, and microelectronics.

**Acknowledgment.** The authors thank Prof. Susan Kauzlarich (Chemistry, UC Davis) for helpful discussions and assistance with conductivity measurements, Prof. William H. Casey (Land, Air and Water Resources, UC Davis) for the use of his atomic force microscope (NSF-EAR94-14103), and the University of California at Davis for financial support.

**Supporting Information Available:** IR spectra and AFM scans for selected nanocomposites (PDF). This material is available free of charge via the Internet at <http://pubs.acs.org>.

## References

- (1) Huang, Y.; Duan, X. F.; Cui, Y.; Lauhon, L. J.; Kim, K. H.; Lieber, C. M. *Science* **2001**, *294*, 1313–1317.
- (2) Tarascon, J. M.; DiSalvo, F. J.; Chen, C. H.; Carroll, P. J.; Walsh, M.; Rupp, L. *J. Solid State Chem.* **1984**, *58*, 290–300.
- (3) Potel, M.; Chevrel, R.; Sergent, M.; Armici, J. C.; Decroux, M.; Fischer, O. *J. Solid State Chem.* **1986**, *35*, 286–290.
- (4) Tarascon, J. M.; Hull, G. W.; DiSalvo, F. J. *Mater. Res. Bull.* **1984**, *19*, 915–924.
- (5) Ajayan, P. M. *Chem. Rev.* **1999**, *99*, 1787–1799.
- (6) Venkataraman, L.; Lieber, C. M. *Phys. Rev. Lett.* **1999**, *83*, 5334–5337.
- (7) Song, J. H.; Messer, B.; Wu, Y. Y.; Kind, H.; Yang, P. D. *J. Am. Chem. Soc.* **2001**, *123*, 9714–9715.
- (8) Golden, J. H.; Disalvo, F. J.; Frechet, J. M. J.; Silcox, J.; Thomas, M.; Elman, J. *Science* **1996**, *273*, 782–784.
- (9) Messer, B.; Song, J. H.; Huang, M.; Wu, Y. Y.; Kim, F.; Yang, P. D. *Adv. Mater.* **2000**, *12*, 1526–1528.
- (10) Song, J. H.; Wu, Y. Y.; Messer, B.; Kind, H.; Yang, P. D. *J. Am. Chem. Soc.* **2001**, *123*, 10397–10398.
- (11) Huynh, W. U.; Dittmer, J. J.; Alivisatos, A. P. *Science* **2002**, *295*, 2425–2427.
- (12) Haremza, J. M.; Hahn, M. A.; Krauss, T. D. *Nano Lett.* **2002**, *2*, 1253–1258.
- (13) Cui, Y.; Wei, Q. Q.; Park, H. K.; Lieber, C. M. *Science* **2001**, *293*, 1289–1292.
- (14) Kong, J.; Chapline, M. G.; Dai, H. J. *Adv. Mater.* **2001**, *13*, 1384–1386.
- (15) Walter, E. C.; Penner, R. M.; Liu, H.; Ng, K. H.; Zach, M. P.; Favier, F. *Surf. Interface Anal.* **2002**, *34*, 409–412.
- (16) Frens, G. *Nature (London) Phys. Sci.* **1973**, *241*, 20.
- (17) Peng, Z. A.; Peng, X. G. *J. Am. Chem. Soc.* **2001**, *123*, 183–184.
- (18) Stipkala, J. M.; Castellano, F. N.; Heimer, T. A.; Kelly, C. A.; Livi, K. J. T.; Meyer, G. J. *Chem. Mater.* **1997**, *9*, 2341–2353.
- (19) Andrew, P.; Barnes, W. L. *Science* **2000**, *290*, 785–788.
- (20) Leung, L. K.; Komplin, N. J.; Ellis, A. B.; Tabatabaie, N. *J. Phys. Chem.* **1991**, *95*, 5918–5924.
- (21) Mott, N. F.; Davis, E. A. *Electronic Processes in Non-Crystalline Materials*; Clarendon Press: Oxford, UK, 1975.
- (22) Wuelfing, W. P.; Murray, R. W. *J. Phys. Chem. B* **2002**, *106*, 3139–3145.
- (23) Kim, S. H.; Medeiros-Ribeiro, G.; Ohlberg, D. A. A.; Williams, R. S.; Heath, J. R. *J. Phys. Chem. B* **1999**, *103*, 10341–10347.
- (24) Golden, J. H.; Disalvo, F. J.; Frechet, J. M. J. *Chem. Mater.* **1995**, *7*, 232–235.
- (25) Golden, J. H.; Disalvo, F. J.; Frechet, J. M. J. *Mater. Sci. Forum* **1994**, *152–153*, 232–235 289–292.

NL025739G